HL-LHC prospects from ATLAS and CMS

Catrin Bernius, on behalf of the ATLAS and CMS Collaborations[1]
SLAC National Accelerator Laboratory, 2575 Sand Hill Rd, Menlo Park, CA 94025, USA
E-mail: catrin.bernius@cern.ch

Abstract. The Large Hadron Collider (LHC) has been successfully delivering proton-proton collision data at the unprecedented center of mass energy of 13 TeV. An upgrade is planned to increase the instantaneous luminosity delivered by the LHC in what is called HL-LHC, aiming to deliver a total of about 3000 fb^{-1} of data per experiment. To cope with the expected data-taking conditions ATLAS and CMS are planning major upgrades of the detectors. Additionally, ATLAS and CMS are preparing inputs to a CERN Yellow Report that aims to summarize the physics reach for HL-LHC and will be submitted as input to the European Strategy before the end of 2018. This contribution focusses on the physics reach expected for a wide range of measurements and searches at the HL-LHC for the ATLAS and CMS experiments, including Higgs coupling, di-Higgs boson production sensitivity, Vector Boson Scattering prospects as well as discovery potential for electroweak SUSY and other exotic benchmark scenarios.

1. Introduction to the HL-LHC

The ATLAS [1] and CMS [2] collaborations at the Large Hadron Collider (LHC) announced the discovery of a 125 GeV Higgs-like boson on 4 July 2012 [3, 4]. Since then, further measurements and studies by both collaborations of the mass [5], the spin and parity [6, 7] as well as the production and decay rates have found no significant deviations from the Standard Model (SM) expectations [8]. In the SM, all properties of the Higgs boson are defined once its mass is known. However, this model leaves many open questions such as the hierarchy problem, regarding the naturalness of the Higgs boson mass, and the nature of the dark matter. Therefore, precise measurements of the Higgs sector are of high priority in the future program of high-energy physics. To be able to extend the successful physics program at the LHC to high precision studies and searches for new physics Beyond the SM (BSM), much more data will need to be collected. To meet this challenge, an extensive upgrade program for the LHC [9] as well as the experiments has been implemented in several phases as shown in Figure 1. The High-Luminosity LHC (HL-LHC) is expected to collect 3000 to 4000 fb^{-1} of data, 10 times more than the integrated luminosity of the LHC Runs 1-3 combined. The HL-LHC baseline parameters with a peak luminosity of 5 to 7×10^{-34} $\text{cm}^{-2}\text{s}^{-1}$ and an average number of pp interactions (pile-up) of 140 to 200 present a very challenging environment to the existing experiments at the LHC.

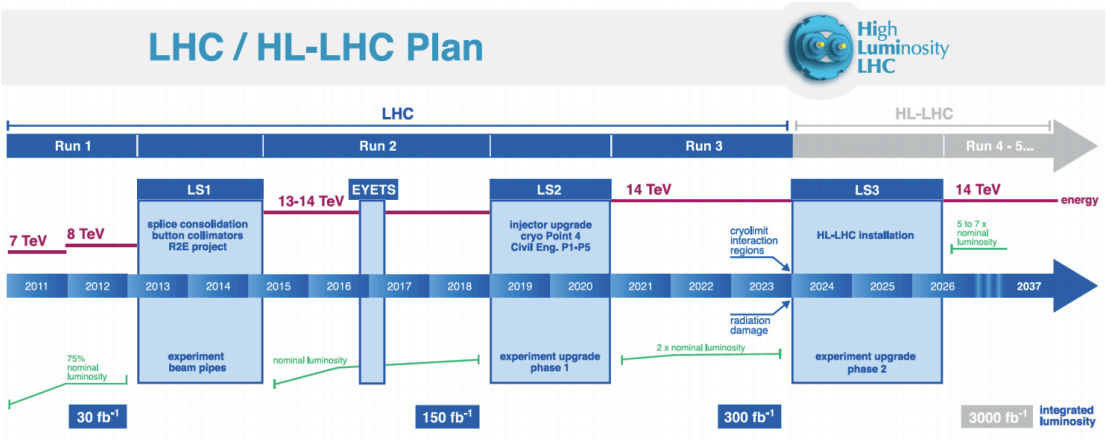

Figure 1. LHC baseline plan for the next decade and beyond in terms of collision energy (upper line) and luminosity (lower lines). The first long shutdown (LS1) 2013-14 is to allow design parameters of beam energy and luminosity. The second one, LS2 in 2018-19, is for securing luminosity and reliability as well as to upgrade the LHC Injectors. After LS3, in 2025 the machine is expected to have the High-Luminosity configuration [9].

2. Detector upgrades for Run 4

To be able to reach the physics goals set for the HL-LHC, both, the ATLAS and CMS detectors have to be upgraded in order to maintain or improve their performance and physics acceptance. A few of these upgrades will be briefly highlighted in the following. More information can be found in the respective references.

2.1. The ATLAS detector

The ATLAS detector will be upgraded to deal with the increased occupancies and data rates. The inner tracking detector will be completely replaced with a new all-silicon Inner Tracker (ITk) [10, 11], increasing the coverage up to a pseudorapidity[2] of $|\eta| = 4$. New Front-End (FE) electronics and a new read-out system in the calorimeters [12, 13] will allow for the read-out of higher resolution objects at the lowest trigger level at an increased rate. In the muon detector system [14], new inner barrel chambers will be installed for increased coverage at the trigger level. A new detector, the high-granularity timing detector [16] will also be installed in the forward region to e.g. separate jets from different pp interactions. The Trigger and Data Acquisition (TDAQ) [15] system will be re-designed making e.g. full granularity detector data available for hardware tracking at a 1 MHz selection rate with the software selection output being 10 kHz.

2.2. The CMS detector

The CMS detector will also undergo major upgrades to be able to cope with the HL-LHC environment. These include a replacement of the silicon strip and pixels in the tracking detector [17] to increase the granularity while reducing material as well as increasing the coverage to $|\eta| = 3.8$. The calorimeter end-caps and FE electronics in the electromagnetic barrel will be replaced for a trigger readout at 40 MHz [18, 19]. The muon system will be, amongst other

[2] ATLAS uses a right-handed coordinate system with its origin at the nominal interaction point (IP) in the centre of the detector and the z-axis along the beam pipe. The x-axis points from the IP to the centre of the LHC ring, and the y-axis points upward. Cylindrical coordinates (r, ϕ) are used in the transverse plane, ϕ being the azimuthal angle around the z-axis. The pseudorapidity is defined in terms of the polar angle θ as $\eta = -\ln\tan(\theta/2)$.

upgrades, extended with new chambers in the forward region, bringing the coverage up to $\eta = 3$ [20]. A minimum ionising particle timing detector [21] will be installed in the central region of the CMS detector to improve the particle-flow performance. Finally also the TDAQ system will undergo upgrades for hardware tracking at 40 MHz with a software selection output of 7.5 kHz [22, 23].

3. Physics prospects at the HL-LHC

Higgs boson physics will be a major component of the extensive physics program at the HL-LHC with the main measurements focussing on Higgs couplings and self-coupling, Higgs differential distributions, rare Higgs decays and heavy Higgs searches. Additionally there is strong support for a rich program in SM and flavour physics as well as for BSM searches. In the following only brief descriptions of selected projections that have been presented will be given. Far more detail can be found in the respective references as well as on the public pages of the ATLAS [24] and CMS [25] experiments. These studies of the assessment of the HL-LHC performance have been carried out as input to the HL-LHC Yellow Report (currently in preparation) as well as the European Strategy Process [26]. In the presented projections, the effects of the upgraded detectors have been taken into account by applying energy smearing, object efficiencies and fake rates to truth level quantities, and following parameterisations based on detector performance studies. An integrated luminosity of 3000 fb^{-1} and an average pile-up of 200 are assumed.

3.1. Higgs self-coupling and HH sensitivity

While many properties of the Higgs boson can be studied with the current LHC dataset, other properties, such as the Higgs self-coupling cannot be extracted from the existing dataset. Even with the large dataset expected at the HL-LHC, measurements of the Higgs self-coupling are expected to be extremely challenging. A direct measurement of the Higgs trilinear self-coupling λ_{HHH} requires the study of the Higgs boson pair productions. For a centre-of-mass energy of 14 TeV, the production cross section of pairs of 125 GeV Higgs bosons is estimated to be 39.6 fb [27].

One of the most promising channels to measure the Higgs self-coupling is the $H(\rightarrow b\bar{b})H(\rightarrow \gamma\gamma)$ final state, for which the results of the ATLAS projection are presented here, with all details of the analysis to be found in Ref. [28], while the CMS projection for the Higgs pair production can be found in Ref. [29]. This channel profits from a clean HH signal extraction thanks to the narrow mass peak of the $H(\rightarrow \gamma\gamma)$ decay. As the low branching ratio (0.13 %) for this decay leads to low expected signal rates, only the gluon-gluon production mode is studied. Following the selection procedure described in Ref. [28], the expected numbers of signal and background events, normalised to an integrated luminosity of 3000 fb^{-1}, are estimated using simulated events.

Figure 2 (right) shows the invariant mass distributions of the diphoton pairs. The dominant backgrounds are non-resonant $b\bar{b}\gamma\gamma$ and $b\bar{b}j\gamma$ final states. Other processes that also contribute significantly to the total expected background include $ZH(\rightarrow \gamma\gamma)$, $t\bar{t}H(\rightarrow \gamma\gamma)$, $c\bar{c}\gamma\gamma$, $b\bar{b}jj$, and $t\bar{t}\gamma$.

Using a cut-based analysis the estimated number of signal events is 9.544 $\pm$ 0.029, to be compared to a background level of 90.9 $\pm$ 2.0 events. The combination of these numbers gives an expected significance of 1.05σ for 3000 fb^{-1}. At 95% CL, the Higgs boson self-coupling is expected to be constrained to $-0.8 < \lambda/\lambda_{\mathrm{SM}} < 7.7$ (see Figure 2 (right)). This is not enough on its own to claim evidence for the observation of Higgs pair production, or to determine whether the Higgs self-coupling strength is close to its SM expectation. This channel is expected to be combined with similar measurements for HH boson production in other decay channels such as $HH \rightarrow b\bar{b}b\bar{b}$ and $HH \rightarrow b\bar{b}\tau\tau$ and to be part of a combination of ATLAS and CMS results.

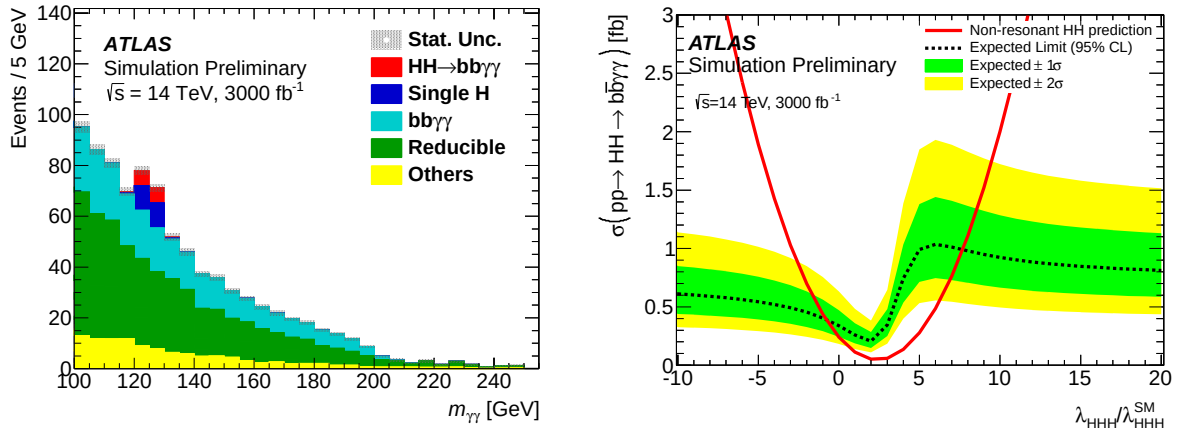

Figure 2. Left: The diphoton invariant mass distribution after all the selection cuts except for the cuts on the diphoton invariant mass for an average number of pile-up events of 200. The shaded area corresponds to the MC statistical uncertainty. Right: Expected 95% CL upper limit on the cross-section $\sigma(HH \rightarrow b\bar{b}\gamma\gamma)$ with 3000 fb^{-1} of data and neglecting systematic uncertainties, as a function of the Higgs self-coupling constant λ in units of λ_{SM}. The $\pm 1\sigma$ and $\pm 2\sigma$ uncertainty bands are shown in green and yellow. The cross-section exclusion limit grows less stringent in the range $3 < \lambda/\lambda_{\mathrm{SM}} < 5$ due to the shift of the number of expected HH events towards lower values where the cross section is decreased. Figures taken from Ref. [28].

The projected sensitivity of various channels for SM HH production is described in detail in Ref. [30]. Figure 3 (left) shows the uncertainty in signal strength $\mu = \sigma/\sigma_{\mathrm{SM}}$, providing different assumptions on the systematic uncertainties which are described in detail in Ref. [30]. It can be seen that the impact of systematics differ across all channels, with the most sensitive being the $H(\rightarrow b\bar{b})H(\rightarrow \gamma\gamma)$ final state. The impact on the significance by assuming different systematic uncertainties can be seen in Figure 3 (right) at hand of the $H(\rightarrow b\bar{b})H(\rightarrow \tau\tau)$ final state. The three scenarios for the assumed uncertainties in this example are: All systematic uncertainties are kept constant with the integrated luminosity and the CMS detector performance is unchanged with respect to the reference analysis (ECFA16 S1); The theoretical uncertainties are scaled down by a factor of 2, while experimental systematic uncertainties are scaled down by the square root of the integrated luminosity until they reach a defined lower limit based on estimates of the achievable accuracy with the upgraded detector (ECFA16 S2); The statistical error only.

3.2. Standard Model physics

One of the physics goals of the HL-LHC is to perform precise SM measurements that require high accuracy and a significant amount of data. This section presents extrapolations for measurements of the top quark mass, based on results obtained mainly at $\sqrt{s} = 8$ TeV, with particular focus on the projected evolution of systematic uncertainties [31]. The top quark is the heaviest known elementary particle. Its mass, m_t, is a fundamental parameter of the SM, affecting predictions in QCD as well as the electroweak sector. It contributes significantly to the quartic Higgs coupling and affects constraints on the stability of the electroweak vacuum, as well as on models with cosmological implications.

Figure 4 summarises the expected precision on m_t for the various measurement techniques that are extensively discussed in Ref. [31]. With data collected during Run 1, most analyses were already limited by systematic uncertainties except for the J/Ψ method which is still affected

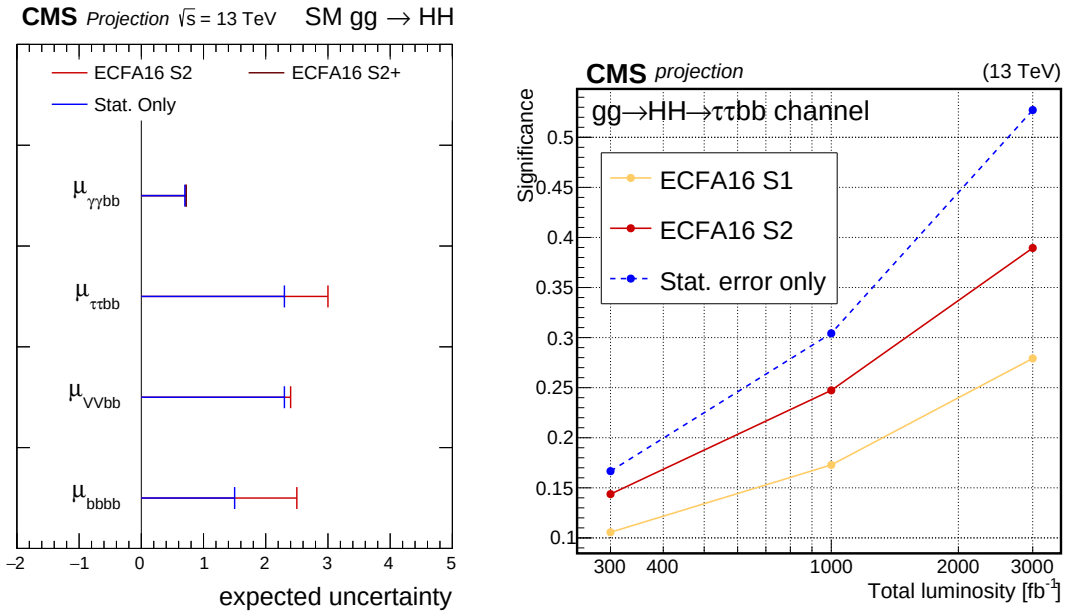

Figure 3. Left: Projection of the sensitivity to the SM $gg \to HH$ production at 3000 fb^{-1}, based on 13 TeV preliminary analyses performed with data collected in 2015. The uncertainty in the signal modifier $\mu = \sigma/\sigma_{\mathrm{SM}}$ is provided assuming different scenarios on the systematic uncertainties. Right: Projection of the sensitivity to the SM $HH \to \tau\tau b\bar{b}$ production as function of the collected luminosity, based on the 13 TeV preliminary analysis performed with data collected in 2015, under different assumptions on the systematic uncertainties. Figures taken from Ref. [30].

by a sizeable statistical uncertainty. The J/Ψ method makes use of a partial reconstruction of top quarks in leptonic final states containing $J/\Psi \to \mu^+\mu^-$ from the b quark fragmentation and determines the top quark mass through its correlation with the mass of the J/Ψ + lepton system (see Ref. [31] for a more detailed description). With 3 ab^{-1} of data, all of the considered analyses will be limited by systematic uncertainties and especially by theoretical modelling uncertainties. The most precise method, the reference method, is expected to yield an ultimate relative precision below 0.1% at HL-LHC. The other techniques are expected to be precise enough to carry significant weight in a combination with the reference method. This would make it possible to further reduce the systematic uncertainties, which are related mostly to the jet energy scale and hard process modelling.

3.3. Supersymmetry searches

In the electroweak sector, the supersymmetric partners of the Higgs, photon, Z, and W are of spin 1/2 that further mix in neutralino ($\tilde{\chi}^0_{1,2,3,4}$) and chargino ($\tilde{\chi}^\pm_{1,2}$) states, also called electroweakinos. In anomaly-mediated supersymmetry breaking (AMSB) scenarios , the supersymmetric partners of the SM W-bosons, the winos, are the lightest gaugino states. In this case, the lightest chargino ($\tilde{\chi}^\pm_1$) and the lightest neutralino ($\tilde{\chi}^0_1$), are both largely composed of the wino eigenstates and are nearly mass-degenerate. Due to this small mass difference, the $\tilde{\chi}^\pm_1$ can have a long enough lifetime such that it decays inside the detector. AMSB scenarios naturally predict a pure wino lightest supersymmetric particle (LSP), which is a dark-matter candidate. Other scenarios following from naturalness arguments suggest the absolute value of the Higgsino mass parameter μ to be near the weak scale such that the Higgsinos should be

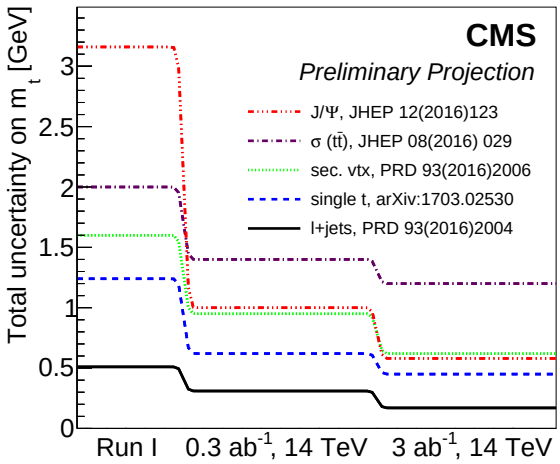

Figure 4. Total uncertainty on the top quark mass (m_t) obtained with different measurement methods and their projections to the HL-LHC. The projections for $\sqrt{s} = 14$ TeV, with 0.3 ab^{-1} or 3 ab^{-1} of data, are based on m_t measurements performed at the LHC Run 1, assuming that an upgraded detector will maintain the same physics performance despite a severe pile-up. Figure taken from Ref. [31].

light, with masses below one TeV, while the magnitude of the bino and wino mass parameters, M_1 and M_2 can be significantly larger, i.e. $|\mu| \ll M_1, M_2$. This results in the three lightest electroweakino states, $\tilde{\chi}_1^0$, $\tilde{\chi}_1^\pm$, $\tilde{\chi}_2^0$ being dominated by the Higgsino component. In this scenario, the three lightest electroweakino masses are separated by hundreds of MeV to tens of GeV depending on the composition of these mass eigenstates, which is determined by the specific values of M_1 and M_2. Investigating either of these scenarios, with very small mass splitting between the lightest electroweakinos, is particularly challenging at hadron colliders, both due to the small cross-sections and due to the small transverse momenta (p_T) of the final state particles. The two searches presented in here investigate electroweakino production in these two, nearly mass degenerate, scenarios assuming an integrated luminosity of 3000 fb^{-1}. In the following, only the results are presented, more details can be found in Ref. [32].

The disappearing track search investigates scenarios where the $\tilde{\chi}_1^\pm$ and $\tilde{\chi}_1^0$ are almost mass degenerate, leading to a long lifetime for the $\tilde{\chi}_1^\pm$ which decays after the first few layers of the inner detector, leaving a track in the innermost layers of the detector. Limits at 95% CL on the chargino lifetime are shown in Figure 5 as a function of the $\tilde{\chi}_1^\pm$ mass. The simplified models of chargino production considered include chargino pair production and chargino-neutralino production (both $\tilde{\chi}_1^\pm\tilde{\chi}_1^\mp$ and $\tilde{\chi}_1^\pm\tilde{\chi}_1^0$). The potential for the full HL-LHC dataset is expected to exclude at the 95% CL chargino lifetimes, assuming a wino-like (higgsino-like) LSP, of between 7 ps (10 ps) and 4 μs (1.5 μs) for light charginos with a mass of 100 GeV. Heavier wino-like (higgsino-like) charginos are expected to be excluded up to $m(\tilde{\chi}_1^\pm) = 1100$ GeV (750 GeV) for lifetimes of 1 ns. The discovery potential of the analysis would allow for the discovery of wino-like (higgsino-like) charginos of mass 100 GeV with lifetimes between 20 ps and 700 ns (30 ps and 250 ns), or for a lifetime of 1 ns would allow the discovery of wino-like (higgsino-like) charginos of mass up to 800 GeV (600 GeV).

The dilepton search investigates final states containing two soft muons and a large transverse momentum imbalance, which arise in scenarios where $\tilde{\chi}_2^0$ and $\tilde{\chi}_1^\pm$ are produced and decay via

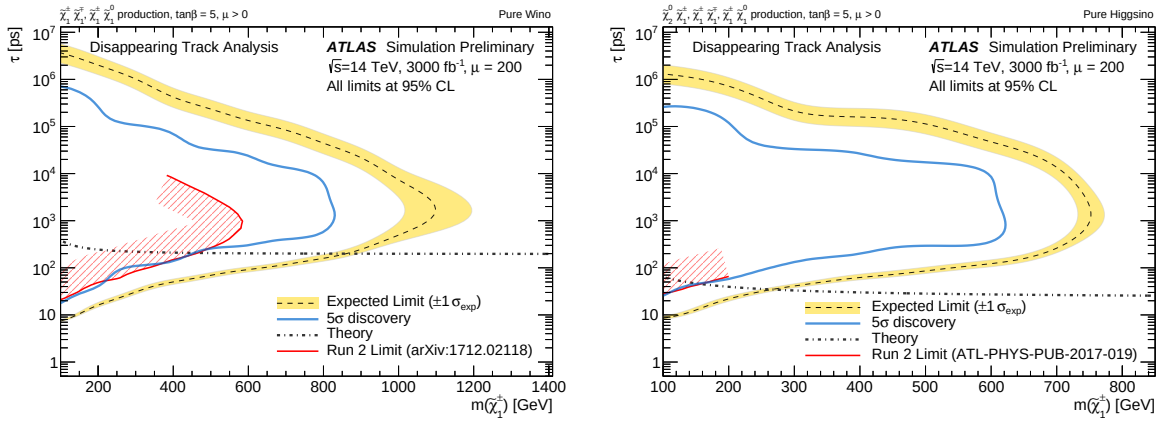

Figure 5. Expected exclusion limits at 95% CL from the disappearing track search using 3000 fb^{-1} of 14 TeV pp collision data as a function of the $\tilde{\chi}_1^{\pm}$ mass and lifetime. Simplified models including both $\tilde{\chi}_1^{\pm}\tilde{\chi}_1^{\mp}$ and $\tilde{\chi}_1^{\pm}\tilde{\chi}_1^0$ are considered assuming pure-wino scenarios (left) and pure-higgsino scenarios (right). The yellow band shows the 1σ region of the distribution of the expected limits. The median of the expected limits is shown by a dashed line. The red line presents the current limits from the Run 2 analysis and the hashed region is used to show the direction of the exclusion. The expected limits with the upgraded ATLAS detector would extend these limits significantly. Figures taken from Ref. [32].

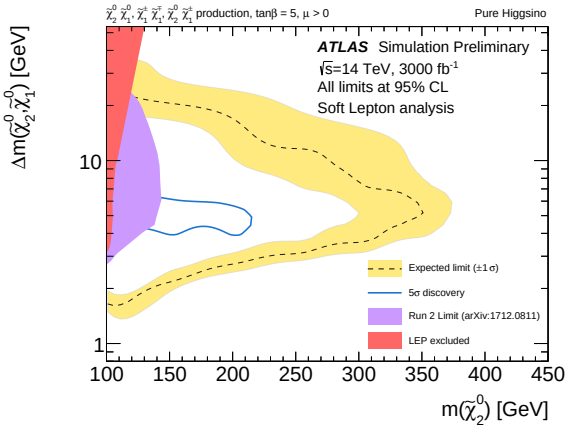

Figure 6. Expected exclusion at the 95% CL from the disappearing track and dilepton searches in the $\Delta m(\tilde{\chi}_2^0, \tilde{\chi}_1^0)$, $m(\tilde{\chi}_2^0)$ mass plane. The blue curve presents the exclusion limits from the dilepton search. The yellow contour presents the exclusion limit from the disappearing track search. The figure also presents the limits on chargino production from LEP. Figure taken from Ref. [32].

an off-shell Z or W boson respectively, $\tilde{\chi}_2^0 \to Z^*\tilde{\chi}_1^0$ and $\tilde{\chi}_1^{\pm} \to W^*\tilde{\chi}_1^0$. Due to the very small mass splitting of the electroweakinos in this scenario, a jet arising from initial-state radiation is required, to boost the sparticle system.

Figure 6 shows the 95% CL expected exclusion limits in the $\Delta m(\tilde{\chi}_2^0, \tilde{\chi}_1^0)$, $m(\tilde{\chi}_2^0)$ plane. With 3000 fb^{-1}, $\tilde{\chi}_2^0$ masses up to 350 GeV could be excluded, as well as $\Delta m(\tilde{\chi}_2^0, \tilde{\chi}_1^0)$ between 2 and 20 GeV for $m(\tilde{\chi}_2^0) = 150$ GeV. In the figure the blue curve presents the 5σ discovery potential of the search.

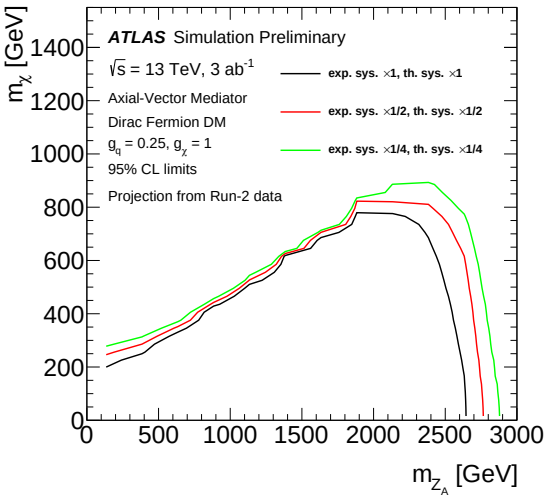

Figure 7. Expected 95% CL excluded regions on the (m_χ, m_{Z_A}) mass plane for the axial-vector simplified model with couplings $g_\chi = 1$ and $g_q = 0.25$, for a luminosity of 3000 fb^{-1}. Three contours are shown in each plot, corresponding to the three different systematic uncertainty scenarios: standard (black), reduced by a factor 2 (red) and 4 (green). Figure taken from Ref. [38].

3.4. Other BSM searches

While there are many BSM searches that will benefit from the HL-LHC dataset and the upgraded detectors, only one additional example from the BSM search sector is giving here. The final state with at least one jet and large missing transverse momentum (E_T^{miss} + jet) is a key channel for the search for dark matter at the LHC. Various theories [33, 34, 35] predict the production of pairs of Weakly Interacting Massive Particles (WIMPs) [36, 37] in association with hadronic jets from initial state radiation which can be used to discriminate signal from background events. This process is described with simplified benchmark models, which assume the existence of a massive mediator of the interaction between the initial state partons and the WIMPs. Depending on the spin-parity state of the mediator and on its couplings, different sensitivity is achieved at the LHC compared to direct and indirect detection experiments, with differing complementarity between LHC search channels, namely those with missing transverse momentum and those with resonant particles. The goal of this study [38] is to evaluate the impact of different assumed systematic uncertainty scenarios on the expected sensitivity to dark matter in the E_T^{miss} + jet channel. A simplified benchmark model is chosen to illustrate the WIMP discovery potential, where Dirac fermion WIMPs, χ, are pair-produced from the s-channel exchange of a spin-1 mediator, Z_A, with axial-vector couplings. The model is defined by four free parameters: the mediator mass (m_{Z_A}), the WIMP mass (m_χ), the coupling strength of the flavour-universal mediator-quark interaction (g_χ), and the coupling strength of the mediator-WIMP interaction (g_q). The exclusion limits, obtained with the profile likelihood method, for each of the three considered systematic uncertainty scenarios is shown in the (m_χ, m_{Z_A}) mass plane in Figure 7. The 95% CL exclusion contour for $m_\chi = 1$ GeV can be extended up to $m_{Z_A} \sim 2.65$ TeV. The excluded region that can be obtained by reducing by a factor two (four) all systematic uncertainties reaches, for low m_χ, mediator masses of about 2.77 (2.88) TeV. Small differences between systematic uncertainty scenarios are observed when approaching the region where the decay of the mediator in two WIMPs is off the mass shell ($m_{Z_A} < 2m_\chi$), due to the decrease of the signal cross-section. The results obtained for the discovery power can be found in Ref. [38].

4. Summary

The HL-LHC provides an unprecedented opportunity to study the Higgs boson in great detail and offers a unique ability to probe new physics beyond the Standard Model. The expected physics reach of the ATLAS and CMS detectors at the HL-LHC era and its discovery potential in the Higgs sector has been studied in detail as input to the Yellow Report that is due to be published in the beginning of 2019.

References

[1] ATLAS Collaboration 2008 *JINST* **3** S08004
[2] CMS Collaboration 2008 *JINST* **3**, S08004
[3] ATLAS Collaboration 2012 *Phys. Lett. B* **716** 1-29
[4] CMS Collaboration 2012 *Phys. Lett. B* **716** 30-61
[5] ATLAS Collaboration, CMS Collaboration 2015 *Phys. Rev. Lett.* **114** 191803
[6] CMS Collaboration 2015 *Phys. Rev. D* **92** 012004
[7] ATLAS Collaboration 2015 *Eur. Phys. J. C* **75** 476
[8] ATLAS Collaboration, CMS Collaboration 2016 *JHEP* **08** 045
[9] G. Apollinari, I. Bjar Alonso, O. Brning, P. Fessia, M. Lamont, L. Rossi, L. Tavian (editors), CERN-2017-007-M, https://cds.cern.ch/record/2284929
[10] ATLAS Collaboration, CERN-LHCC-2017-021, https://cds.cern.ch/record/2285585
[11] ATLAS Collaboration, CERN-LHCC-2017-005, https://cds.cern.ch/record/2257755
[12] ATLAS Collaboration, CERN-LHCC-2017-018, https://cds.cern.ch/record/2285582
[13] ATLAS Collaboration , CERN-LHCC-2017-019, https://cds.cern.ch/record/2285583
[14] ATLAS Collaboration, CERN-LHCC-2017-017, https://cds.cern.ch/record/2285580
[15] ATLAS Collaboration, CERN-LHCC-2017-020, https://cds.cern.ch/record/2285584
[16] ATLAS Collaboration, CERN-LHCC-2018-023, https://cds.cern.ch/record/2623663
[17] CMS Collaboration, CERN-LHCC-2017-009, https://cds.cern.ch/record/2272264
[18] CMS Collaboration, CERN-LHCC-2017-011, https://cds.cern.ch/record/2283187
[19] CMS Collaboration, CERN-LHCC-2017-023, https://cds.cern.ch/record/2293646
[20] CMS Collaboration, CERN-LHCC-2017-012, https://cds.cern.ch/record/2283189
[21] CMS Collaboration, CERN-LHCC-2017-027, https://cds.cern.ch/record/2296612
[22] CMS Collaboration, CERN-LHCC-2017-013, https://cds.cern.ch/record/2283192
[23] CMS Collaboration, CERN-LHCC-2017-014, https://cds.cern.ch/record/2283193
[24] ATLAS Collaboration, https://twiki.cern.ch/twiki/bin/view/AtlasPublic/UpgradePhysicsStudies
[25] CMS Collaboration, http://cms-results.web.cern.ch/cms-results/public-results/preliminary-results/FTR
[26] European Strategy for Particle Physics, https://europeanstrategy.cern/european-strategy-for-particle-physics
[27] D. de Florian et al., 2016 Handbook of LHC Higgs Cross Sections: 4. Deciphering the Nature of the Higgs Sector, arXiv:1610.07922 [hep-ph]
[28] ATLAS Collaboration, ATL-PHYS-PUB-2017-001, https://cds.cern.ch/record/2243387
[29] CMS Collaboration, CMS-PAS-FTR-15-002, https://cds.cern.ch/record/2063038
[30] CMS Collaboration, CMS-PAS-FTR-16-002, https://cds.cern.ch/record/2266165
[31] CMS Collaboration, CMS-PAS-FTR-16-006, https://cds.cern.ch/record/2262606
[32] ATLAS Collaboration, ATL-PHYS-PUB-2018-031, https://cds.cern.ch/record/2647294
[33] J. Abdallah et al., 2015 *Phys. Dark Univ.* **9-10** 8-23
[34] D. Abercrombie et al., 2015 Dark Matter Benchmark Models for Early LHC Run-2 Searches: Report of the ATLAS/CMS Dark Matter Forum, arXiv:1507.00966 [hep-ex]
[35] O. Buchmueller, M. J. Dolan, S. A. Malik and C. McCabe, 2015 *JHEP* **01** 037
[36] G. Steigman and M. S. Turner, 1985 *Nucl. Phys. B* **253** 375
[37] E. W. Kolb and M. S. Turner, 1990 *Front. Phys.* **69** 1
[38] ATLAS Collaboration, ATL-PHYS-PUB-2018-043, https://cds.cern.ch/record/2650050